

Junction Surface Recombination Concept as Applied to Silicon Solar Cell Maximum Power Point Determination Using Matlab/Simulink: Effect of Temperature

Bakary Dit Dembo Sylla¹, Ibrahima Ly², Ousmane Sow³,
Babou Dione¹, Youssou Traore¹, Grégoire Sissoko¹

¹Laboratory of Semiconductors and Solar Energy, Physics Department, Faculty of Science and Technology, University Cheikh Anta Diop, Dakar, Senegal

²Electromechanical department, Polytechnic School of Thiès, Thiès, Senegal

³University Institute of Technology, University of Thiès, Thiès, Senegal

Email: gsissoko@yahoo.com

How to cite this paper: Sylla, B.D.D., Ly, I., Sow, O., Dione, B., Traore, Y. and Sissoko, G. (2018) Junction Surface Recombination Concept as Applied to Silicon Solar Cell Maximum Power Point Determination Using Matlab/Simulink: Effect of Temperature. *Journal of Modern Physics*, 9, 172-188. <https://doi.org/10.4236/jmp.2018.92011>

Received: December 15, 2017

Accepted: January 16, 2018

Published: January 19, 2018

Copyright © 2018 by authors and Scientific Research Publishing Inc. This work is licensed under the Creative Commons Attribution International License (CC BY 4.0).

<http://creativecommons.org/licenses/by/4.0/>



Open Access

Abstract

In this work, we study the method for determining the maximum of the minority carrier recombination velocity at the junction $S_{f_{max}}$ corresponding to the maximum power delivered by the photovoltaic generator. For this, we study the temperature influence on the behavior of the front white biased solar cell in steady state. By solving the continuity equation of excess minority carrier in the base, we have established the expressions of the photocurrent density, the recombination velocity on the back side of the base S_b , and the photovoltage. The photocurrent density and the photovoltage are plotted as a function of S_f , called, minority carrier recombination velocity at the junction surface, for different temperature values. The illuminated I-V characteristic curves of the solar cell are then derived. To better characterize the solar cell, we study the electrical power delivered by the base of the solar cell to the external charge circuit as either junction surface recombination velocity or photovoltage dependent. From the output power versus junction surface recombination velocity S_f , we have deduced an eigenvalue equation depending on junction recombination velocity. This equation allows to obtain the maximum junction recombination velocity $S_{f_{max}}$ corresponding to the maximum power delivered by the photovoltaic generator, throughout simulink model. Finally, we deduce the conversion efficiency of the solar cell.

Keywords

Silicon Solar Cell-Junction Surface Recombination Velocity-Maximum Power

1. Introduction

Many techniques exist and provide photovoltaic generators to operate at maximum points of their characteristics [1] [2]. The method used in this work enables us to determine the maximum power point based on electronic transport parameters of the solar cell. Contrary to the most commonly used MPPT technical, which takes into account the controllers particularly adapted for managing a non-linear source by forcing the generator to work at its maximum power point (MPP) [3] [4] [5].

This study aims to determination of the maximum power point supplied by a photovoltaic generator in static regime under the effect of temperature. For this, we give through the continuity equation, the expressions of minority carrier generation rate, and the density of the excess minority carrier in the base [6] [7].

The expressions of the photocurrent density, the photovoltage, the recombination velocity of the minority carrier at the back surface S_b and the electrical power, all depending on temperature are produced and graphically represented as function of minority carrier recombination velocity at the junction [8] [9] [10].

The $I(S_f)$ - $V(S_f)$ characteristic curves of the photocurrent density as function of photovoltage, the power as a function of minority carrier recombination velocity at the junction or photovoltage dependent, have also graphically represented [11] [12] [13].

A transcendental equation giving the minority carrier recombination velocity to the maximum power points $S_{f_{max}}$ is determined. It is graphically represented by matlab/Simulink as a minority carrier recombination velocity at the junction S_f (Time (secs)). Finally, the graphical results are compared with those of the model [14] [15] [16].

2. Theory

Consider a crystalline silicon solar cell (n^+ - p - p^+). Its structure is illustrated in **Figure 1**.

z is the depth in the base of the solar cell measured from the junction emitter-base ($z = 0$) to the back surface ($z = H$). H is the base thickness.

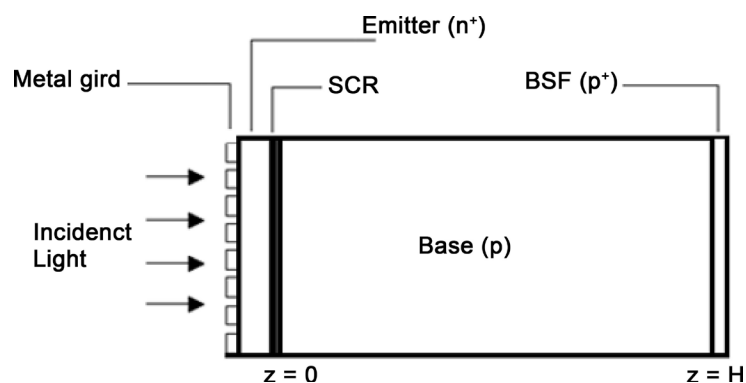


Figure 1. Structure of the silicon solar cell (n^+ - p - p^+) [17].

For a given illumination of the solar cell, different processes take place in the base, it is the absorption of the light, the minority carrier generation, bulk and surfaces recombination and diffusion. These processes can be simplified to the one dimensional continuity equation with boundary conditions:

$$\frac{\partial^2 \delta(z, T)}{\partial z^2} - \frac{\delta(z, T)}{L^2(T)} = -\frac{1}{D(T)} \cdot G(z) \tag{1}$$

$\delta(z, T)$ represents the excess minority carrier density in the solar cell base at position z .

With

$$L(T) = \sqrt{\tau \cdot D(T)} \tag{2}$$

$L(T)$ is the minority carrier diffusion length in the base and is function of the temperature. It also represents the average distance traveled during the lifetime (τ) by the minority carrier before their recombination.

$D(T)$ is the electron diffusion coefficient in the base given by the well-known Einstein relation [18], temperature dependent, given as:

$$D(T) = \mu(T) \frac{K_b}{q} T \tag{3}$$

$\mu(T)$ is the mobility coefficient for electron and depends on the temperature [19], its expression is given by the following equation:

$$\mu(T) = 1.43 \times 10^9 T^{-2.42} \text{ cm}^2 \cdot \text{V}^{-1} \cdot \text{s}^{-1} \tag{4}$$

K_b is the Boltzmann constant, q is the elementary charge of an electron.

$G(z)$ is the minority carriers generation rate at position z in the base, given by [20] [21].

$$G(z) = \sum_{i=1}^3 a_i e^{-b_i \cdot z} \tag{5}$$

The coefficient a_i and b_i are obtained from tabulated values of the radiation in A.M 1.5 condition [22].

The excess minority carrier density is obtained from differential Equation (1) resolution and is given by.

$$\delta(z, T) = A \cdot \cosh\left(\frac{z}{L(T)}\right) + B \cdot \sinh\left(\frac{z}{L(T)}\right) - \sum_{i=1}^3 K_i \cdot e^{-b_i \cdot z} \tag{6}$$

The coefficients A and B are obtained with the boundary conditions at the emitter-base junction and at the back surface of the cell [22] [23]:

i) At the junction: emitter-base ($z = 0$)

$$\left. \frac{\partial \delta(z, T)}{\partial z} \right|_{z=0} = \frac{Sf}{D(T)} \delta(z = 0, T) \Big|_{z=0} \tag{7}$$

ii) At the back side ($z = H$)

$$\left. \frac{\partial \delta(z, T)}{\partial z} \right|_{z=H} = -\frac{Sb}{D(T)} \delta(z = H, T) \Big|_{z=H} \tag{8}$$

Sf is the excess minority carrier recombination velocity at the junction emitter-base, it also characterizes the operating point of the solar cell [24] [25] on the illuminated current-voltage characteristic.

Sb is the excess minority carrier recombination velocity on the back of the base [25]. Its expression is obtained from the derivative (Figure 2) of the photocurrent density for large Sf values [17] [18] [19] [20].

$$\left[\frac{\partial J_{ph}}{\partial Sf} \right] = 0 \tag{9}$$

From the Equation (9), Sb is then expressed as dependent on the following parameters $L(T)$, $D(T)$, $\mu(T)$, b_i and H :

$$Sb(T) = \frac{D(T)}{L(T)} \cdot \sum_{i=1}^3 \frac{L(T) \cdot b_i \left(e^{b_i \cdot H} - \cosh\left(\frac{H}{L(T)}\right) \right) - \sinh\left(\frac{H}{L(T)}\right)}{L(T) \cdot b_i \cdot \sinh\left(\frac{H}{L(T)}\right) + \cosh\left(\frac{H}{L(T)}\right) - e^{b_i \cdot H}} \tag{10}$$

2.1. Photocurrent Density

The expression of the photocurrent density is obtained from the density of the minority charge carriers in the base. It's given by the following relation:

$$J_{ph}(Sf, T) = q \cdot D(T) \cdot \left[\frac{\partial \delta(z, Sf, T)}{\partial z} \right]_{z=0} \tag{11}$$

Figure 2 represents the photocurrent density profile as function of the junction

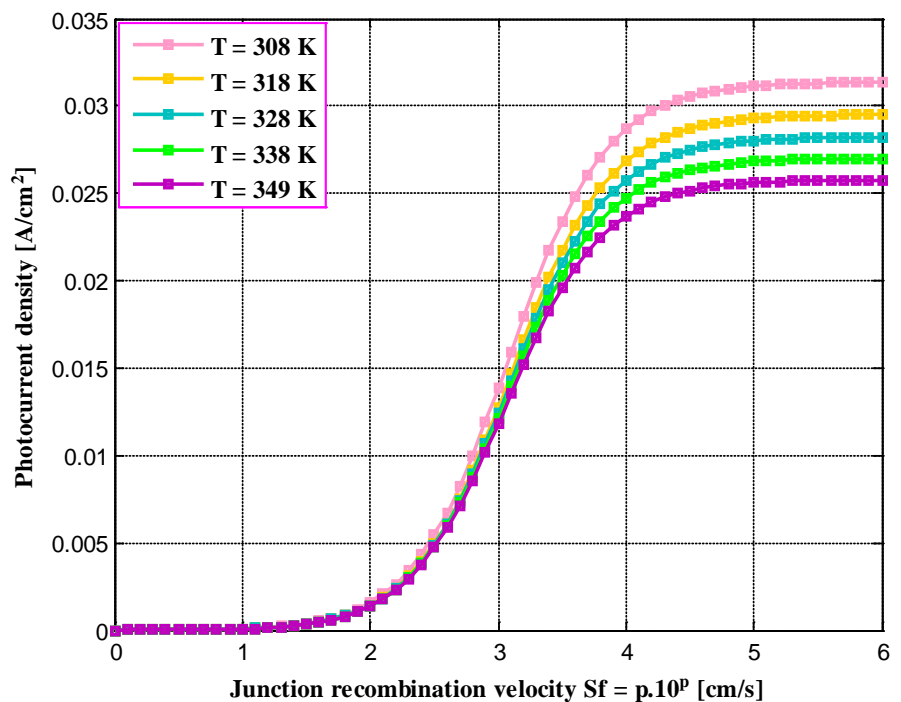


Figure 2. Photocurrent density versus junction recombination velocity for different temperature values.

recombination velocity for different temperature values.

On this curve, the photocurrent density is very low in the vicinity of the open-circuit ($Sf < 2 \times 10^2$ cm/s), then increases very rapidly with the junction minority carrier recombination velocity to reach an asymptotic value at large Sf values ($Sf > 5 \times 10^5$ cm/s) corresponding to solar cell short-circuit photocurrent density. The short circuit current density decreases as the temperature increases. This decreasing due to the disordered movement of the charge carriers because the increasing of temperature causes a thermal agitation.

2.2. Photovoltage

The expression of the photovoltage at the terminal of the solar cell, when the latter is subjected to a multispectral illumination, is obtained by the Boltzmann relation [26].

$$V_{ph}(Sf, T) = V_T \cdot \log \left[\frac{N_b}{n_i^2(T)} \delta(Sf, T) + 1 \right] \quad (12)$$

V_T is the thermal voltage, it is given as follows:

$$V_T = \frac{K_b T}{q} \quad (13)$$

T is the absolute temperature, it's included between 300 - 350 K.

N_b is the acceptor atom doping rate in the base.

$$n_i^2(T) = A \cdot T^3 \cdot \exp \left(-\frac{E_g}{K_b \cdot T} \right) \quad (14)$$

$n_i(T)$ is the law of conservation (generation rate must be equal to recombination rates of charge carriers $n = p = n_i$) [27] [28].

E_g is the energy gap, it corresponds to the difference between the energy of the conduction band E_c and the valence band E_v . $E_g = 1.12 \times 1.6 \times 10^{-19}$ J,

A is a specific constant of the material, $A = 3.87 \times 10^{16} \text{ cm}^{-3} \cdot \text{K}^{-3/2}$ [18].

Figure 3 represents the photovoltage as function of junction recombination velocity for different temperature values.

Figure 3 shows that, at low junction minority carrier recombination velocity values, the photovoltage is maximal and constant, and corresponds to the open-circuit voltage (vicinity of the open-circuit). There is a blockage and storage of minority carriers at the junction. The photovoltage decreases for large junction minority carrier recombination velocity values and it becomes low in the vicinity of the short-circuit (large Sf values), thus the minority carriers crossed over the junction and participate to the production of photocurrent. The increasing of temperature leads to a slight increase in the creation of electron - hole pairs.

2.3. Study of the $I(Sf)$ - $V(Sf)$ Characteristic

The profile of the $I(Sf)$ - $V(Sf)$ characteristic for different temperature values is represented on **Figure 4**.

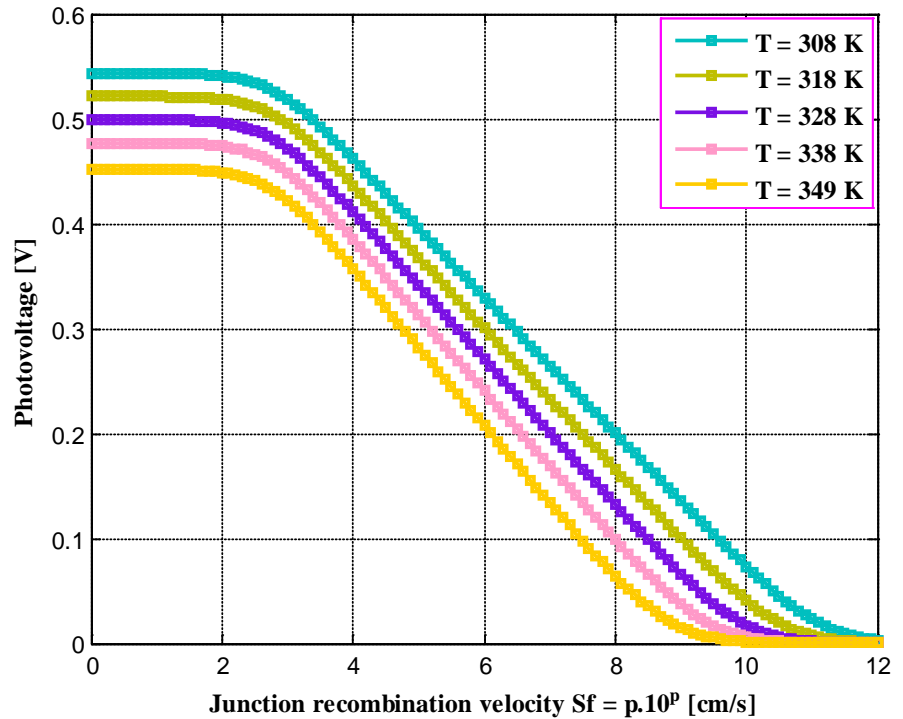


Figure 3. Photovoltage versus junction recombination velocity for different temperature values.

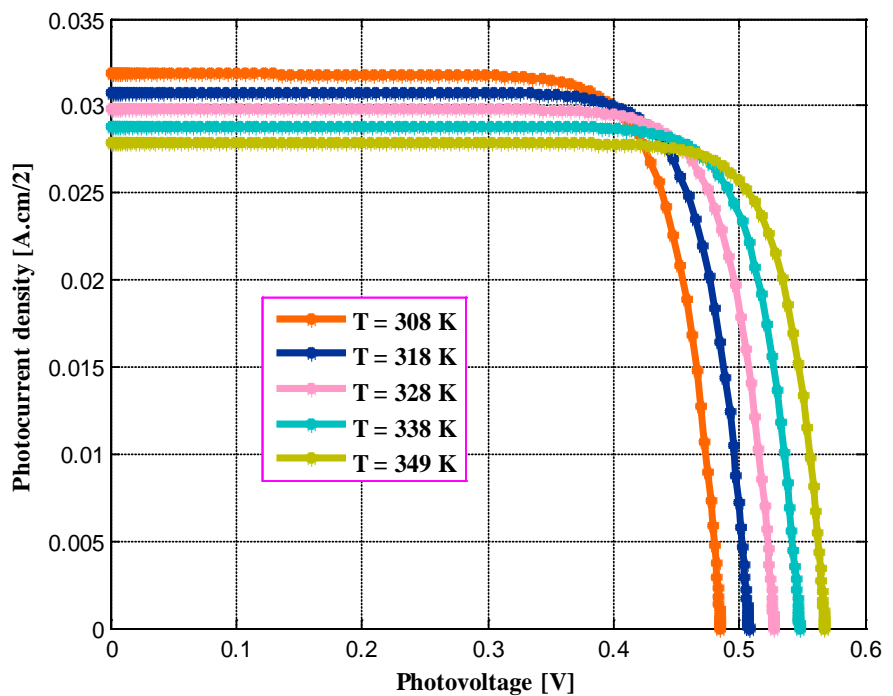


Figure 4. Photocurrent density versus photovoltage for different temperature values.

We notice that, the short-circuit photocurrent density decreases when the temperature increases and the open circuit voltage increases with increasing of temperature.

2.4. Study of the Power and the Maximum Power Point

2.4.1. Study of the Power

The equivalent electrical circuit of an actual solar cell under illumination is represented by **Figure 5**. This circuit treats the solar cell as an ideal current generator which sells a photocurrent density depending on the illumination, connected in parallel with a diode and a shunt resistance R_{sh} and in series with a series resistance R_s .

The Ohm law applied to **Figure 5**, allows to extract the solar cell base electrical power issued to the external charge circuit as following (15):

$$P(Sf, T) = V_{ph}(Sf, T) \cdot I(Sf, T) \quad (15)$$

Applying the first law of Kirchhoff to the circuit of **Figure 5**, the current density supplied to the external charge circuit is given by the following relation [16].

$$I(Sf, T) = I_{ph}(Sf, T) - I_d(Sf, T) - I_{sh}(Sf, T) \quad (16)$$

I_d is the diode current density, its expression is given by the following relation:

$$I_d(Sf, T) = q \cdot Sf_0 \cdot \frac{(n_i(T))^2}{N_b} \cdot \exp\left(\frac{V_{ph}(Sf, T)}{V_T} - 1\right) \quad (17)$$

I_{sh} is the shunt current density, in the case of an ideal current generator, (R_{sh} tends to infinity; $I_{sh} = 0$).

Sf_0 is the intrinsic junction recombination velocity associated with the losses of charge carriers induced by shunt resistance. It characterizes the good quality of the solar cell [29].

Figure 5 and **Figure 6** represent the variations of the electrical power in function of the recombination velocity of the charge carriers at the junction and the photovoltage for different temperature values.

Figure 5 shows that, the power increases with the junction surface recombination velocity until a value Sf_{max} then it decreases. The maximum power point varies with the temperature. Increasing photocurrent density is due to a decreasing of the energy larger band gap E_g . At the same time, we observe an increasing of the diode current density resulting a decreasing values of temperature.

2.4.2. Maximum Power Point and Efficiency

The maximum power point of a generator photovoltaic corresponds to the

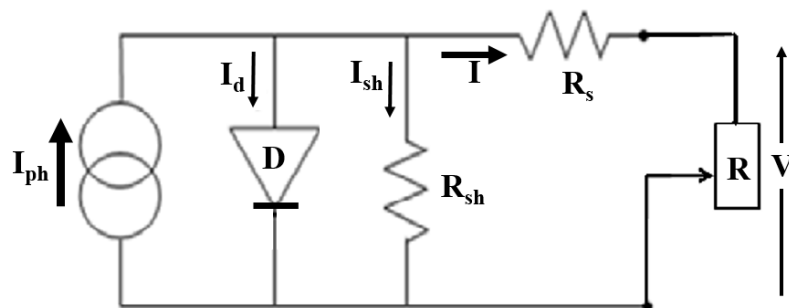


Figure 5. Equivalent electrical circuit of a solar cell [17].

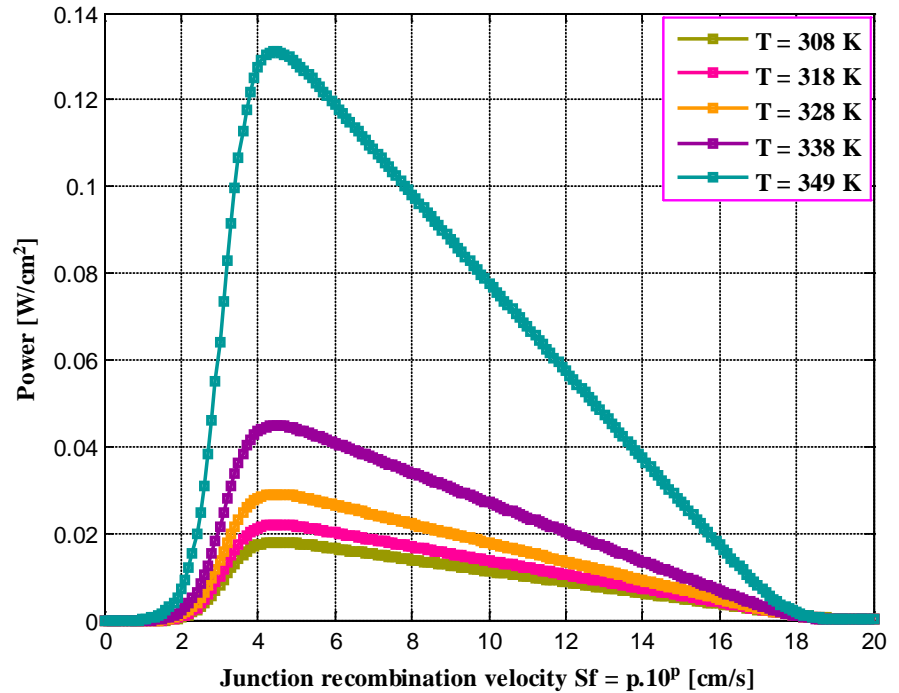


Figure 6. Solar cell power versus junction recombination velocity for different temperature values.

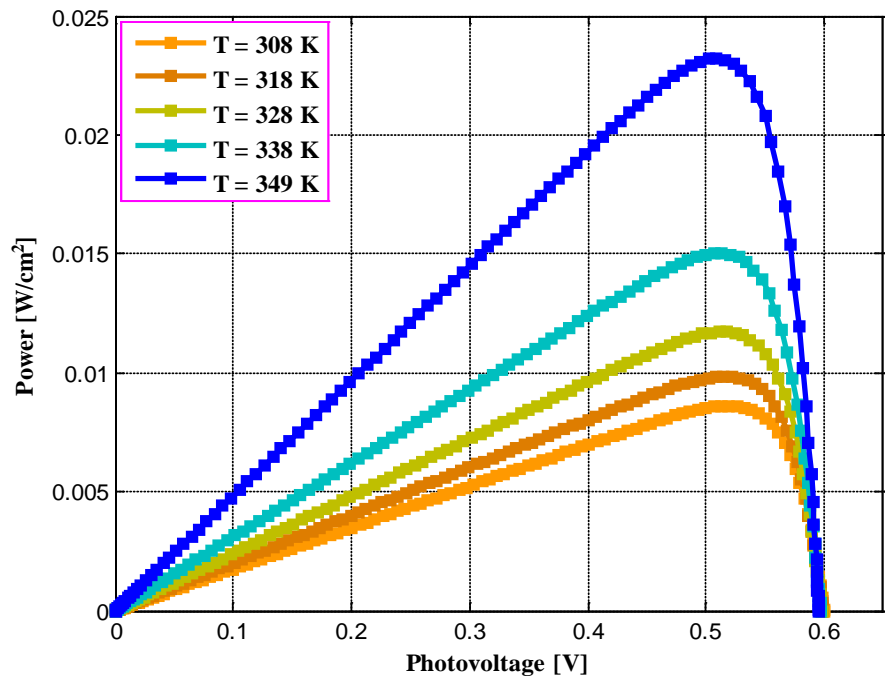


Figure 7. Solar cell power versus photovoltage for different temperature values.

photocurrent density-photovoltage couple generating the maximum electrical power of this solar cell.

Four essential data can be used to determine the photocurrent density-photovoltage characteristic of the photovoltaic generator [17].

- The photocurrent density of short-circuit noted J_{sc}
- The open-circuit voltage noted V_{oc}
- The maximal photocurrent density noted J_{phmax}
- The maximal photovoltage noted V_{phmax}

The product of the maximal photocurrent density and the maximal photovoltage $J_{phmax} \times V_{phmax}$ gives a maximal power P_{max} .

We determine the maximal minority carrier recombination velocity at the junction corresponding to the maximal power point [30] [31]. Let:

$$\frac{\partial P}{\partial Sf} = 0 \tag{18}$$

Let Sf_{max} denote this maximal junction recombination velocity corresponding to the maximal power point. It depends on:

- electronic transport parameters ($L, \mu, D, Sf, Sb, \tau, n_p, N_b$) in the solar cell that are related to physical phenomena,
- geometrical one (H), *i.e.* in the 1D model
- material absorption coefficients (b_i).

All these parameters are taking into account for the determination of the maximum power based on electron diffusion coefficient variation with temperature and the solar cell thickness H [18].

From the Equation (18), the calculation gives the transcendental equation dependent of the junction minority carrier recombination velocity.

and the temperature. It's given by the following expressions:

With

$$M(Sf, T) = \frac{1}{Sf_{max} L} \left[1 - \frac{Sf_{max} L}{Y_1 D + Sf_{max} L} \right] \tag{19}$$

And

$$N(Sf, T)$$

$$= \left[\frac{\Gamma_{max}(0, T)}{\left(\Gamma_{max}(0, T) + \frac{n_i^2}{N_b} \right) \cdot (Sf_{max} \cdot L + Y_1 \cdot D)} \right] * \left[\frac{1}{\log \left(\frac{N_b \cdot \Gamma_{max}(0, T)}{n_i^2} + 1 \right)} \right] \tag{20}$$

$\Gamma_{max}(0, T)$ is the density of the minority carrier on maximum power point, its expression is given by the following relation:

$$\Gamma_{max}(0, T) = K \cdot D \cdot \left[\frac{Y_2 + Y_1 - b_i \cdot L}{Sf_{max} \cdot L + Y_1 \cdot D} \right] \tag{21}$$

With

$$K = \frac{n \cdot a_i \cdot L^2 \cdot \cos(\theta)}{D \cdot (L^2 \cdot b_i^2 - 1)} \tag{22}$$

$$Y_1 = \frac{D/L \cdot \sinh(H/L) + Sb \cdot \cosh(H/L)}{D/L \cdot \cosh(H/L) + Sb \cdot \sinh(H/L)} \tag{23}$$

$$Y_2 = \frac{(D \cdot b_i - Sb) \cdot \exp(-b_i \cdot H)}{D/L \cdot \cosh(H/L) + Sb \cdot \sinh(H/L)} \quad (24)$$

For the transcendental equation modelling a simulink model is used [32] [33]. This model is composed of an inputs block that includes a system allowing to define the set simulation type, simulation parameters, and preferences (powergui), the ramp block, which output a ramp signal starting at the specified time with the start time and initial output estimated at zero. To file block, allows the variable may be created as a matlab time series, an array, or a matlab structure. We used matlab time series which is used for any data type. It also allows defining the decimation and the sample time (-1 for inherited). The constant block containing the different values of temperature. The Sf_{max} block containing the expression of the transcendental equation. Finally, the output block composed of a creator bus, this block creates a bus signal from its inputs, it also allows defining the inherit bus signal names from input ports, the number of inputs, the signal in the bus and the output data type. The time scope block, this block defined the number of input ports (two in this model), input processing: elements as channels (sample based), time span of Sf_{max} block (10 seconds), the time units in metric (based on time span), the time displays ofset at zero, show time axis-labels, the minimum and maximum limit of y-axis and y-axis label.

The model of the transcendental equation is represented in **Figure 8** as follows:

The graphical resolution of this model provides the values of Sf_{max} defined by the intercept point of two curves represented on **Figure 9**. To each operating point generating the maximum electrical power delivered by the photovoltaic generator corresponds to a Sf_{max} value.

Figure 9 shows the increasing of the Sf_{max} values then the temperature increases. Reflecting the increasing of the maximal power as the temperature increases.

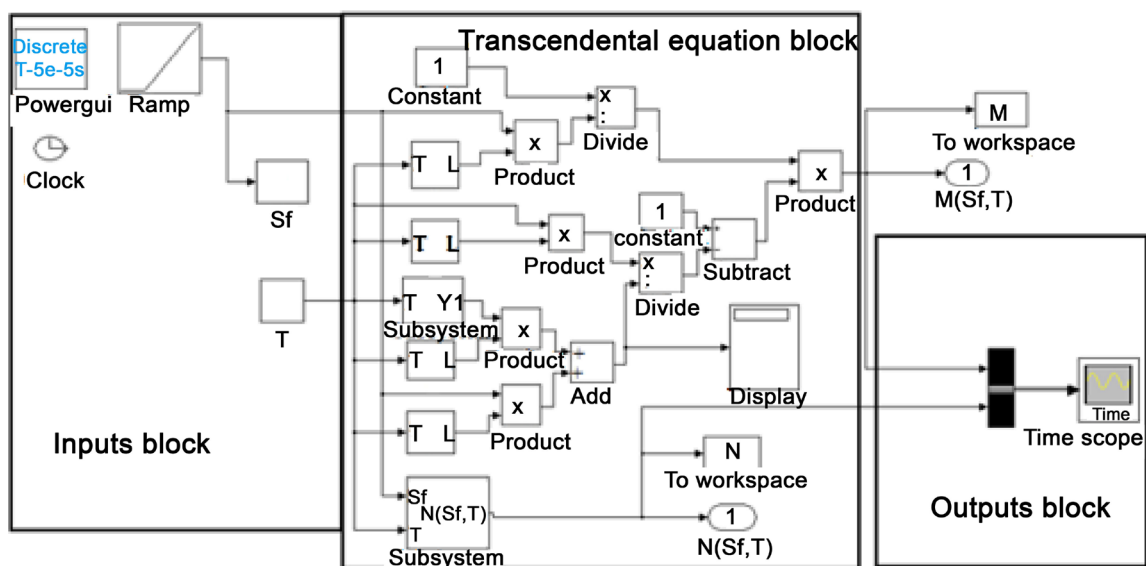


Figure 8. Simulink model of eigenvalue equation.

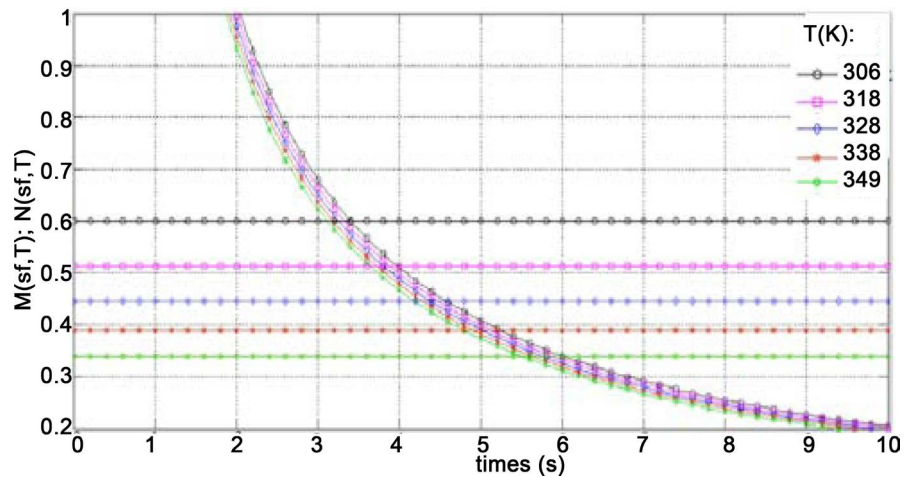


Figure 9. Graphical representation of simulink model of transcendental equation versus junction surface recombination velocity for different temperature values.

Table 1. The numerical values of Sf_{max} corresponding to the maximal power point for different temperature values.

Temperature (K)	Points of intersection for each given temperature values p (cm/s)	Sf_{max} (cm/s)
308 K	3.396	2.443×10^3
318 K	3.883	7.620×10^3
328 K	4.370	23.659×10^3
338 K	4.913	80.909×10^3
349 K	5.501	31.686×10^4

We observe the intercept points on the figure corresponding to the Sf_{max} values. These Sf_{max} values correspond to an operating condition of the solar cell at the maximum power point.

The results obtained by the model on **Figure 9** corresponding the numerical values of Sf_{max} for each maximal power point are given in **Table 1**.

The influence of Sf_{max} on the temperature can be plotted from a theoretical model of Sf_{max} given by the following expression (25):

$$Sf_{max} = b \cdot e^{aT} \tag{25}$$

The resolving of the right equation from **Figure 10** provides the coefficients a and b values follows as: $a = 0.052 \text{ cm}\cdot\text{s}^{-1}/\text{K}$, this value represents the slope corresponding to the vertical variation versus the horizontal variation of the right and $b = 3.216 \text{ cm/s}$ corresponding a temperature of 305 K, it is determined from the y intercepts and it is homogeneous to a maximal surface recombination velocity Sf_{max} . Sf_{max} increases with temperature on a low positive slope.

2.4.3. The Efficiency

The conversion efficiency of the solar cell is a ratio between the maximal power supplied by the solar cell and the absorbed incident light power, writing as follows:

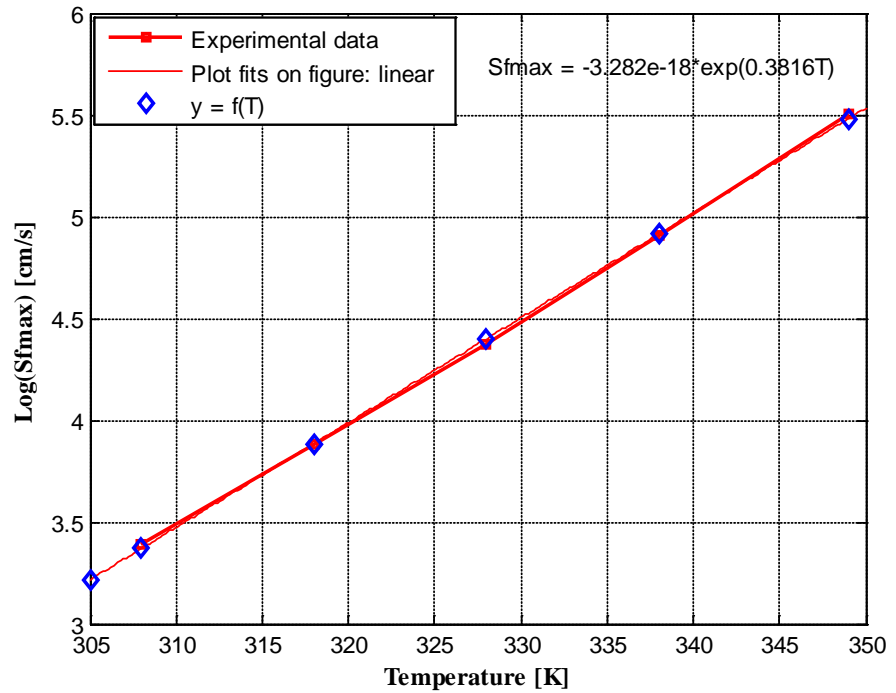


Figure 10. Sf_{max} representation versus temperature.

Table 2. The photocurrent density I_{max} values, the photovoltage V_{max} , the power P_{max} and the efficiency η_{max} corresponding to the maximal power point for different temperature values.

Temperature (K)	308 K	318 K	328 K	338 K	349 K
I_{max} (mA/cm ²)	0.03236	0.03132	0.03033	0.02935	0.02836
$I_d(Sf_{max})$ (mA)	3.023×10^{-4}	2.923×10^{-4}	2.83×10^{-4}	2.741×10^{-4}	2.65×10^{-4}
V_{max} (mV)	0.4891	0.5113	0.5314	0.5514	0.5713
P_{max} (W/cm ²)	0.015679	0.015864	0.015967	0.016032	0.016051
η_{max} (%)	15.679	15.864	15.967	16.032	16.051

$$\eta = \frac{J_{max} \cdot V_{max}}{P_{incident}} \tag{26}$$

$P_{incident}$ is the absorbed incident light power by the solar cell, with $P_{incident} = 100$ mW/cm² in the standards AM 1.5 condition [22].

For representation of efficiency, we have deduced on the characteristic curve of the photocurrent density as function of photovoltage according to Figure 4, the graphical values corresponding to the maximal power point, the maximal photocurrent density, the maximal photovoltage, the maximal power and the maximal conversion efficiency of the solar cell for different temperature values. These results are given in Table 2.

Figures 11-13 represent the maximal photocurrent density I_{max} , the maximal photovoltage V_{max} and the maximal conversion efficiency η_{max} of the solar cell as function of temperature.

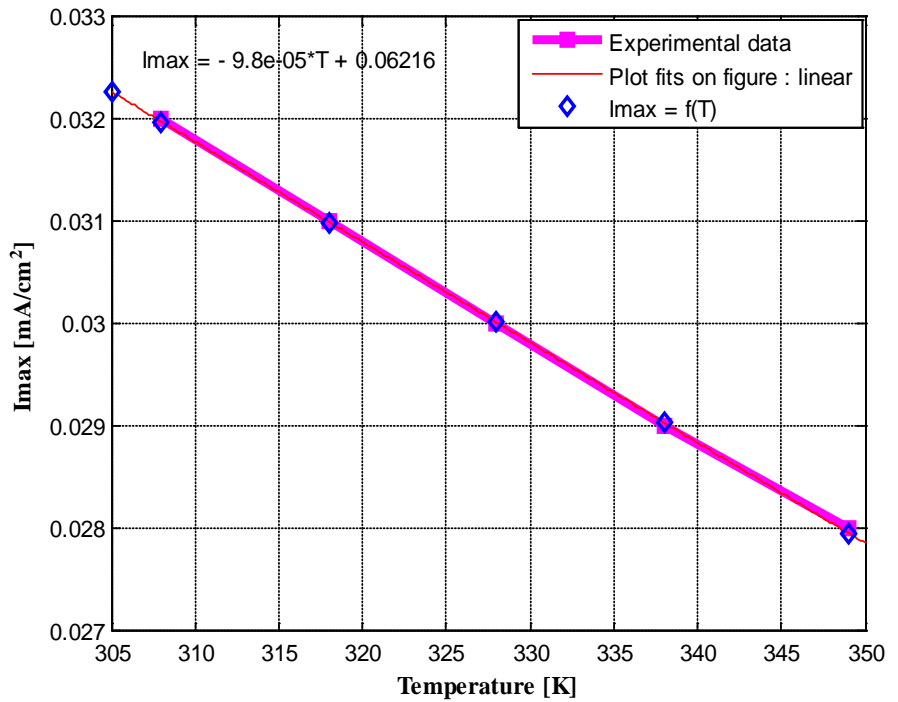


Figure 11. The maximal photocurrent versus temperature.

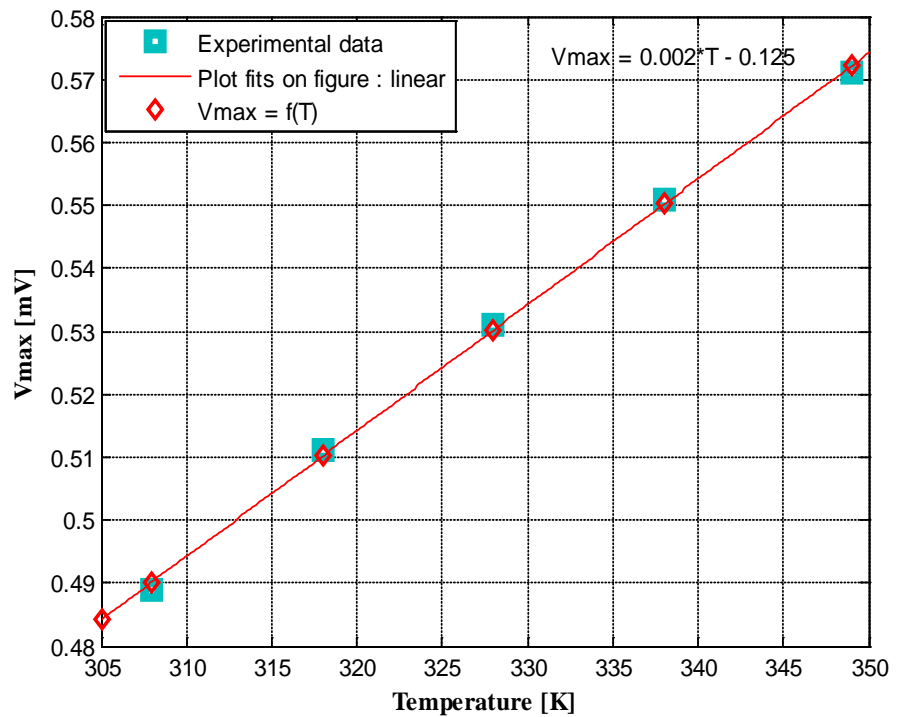


Figure 12. The maximal photovoltage versus temperature.

The resolution of line equation $y = \gamma T + \chi$, allows to obtain the line coefficient γ and χ from Figure 11, with $\gamma = -9.756 \times 10^{-5} \text{ mA}\cdot\text{cm}^{-2}/\text{K}$ and $\chi = 0.03227 \text{ mA}/\text{cm}^{-2}$ corresponding at the temperature of 305 K. On this curve, we notice a decreasing of the maximal photocurrent I_{max} when the temperature increases,

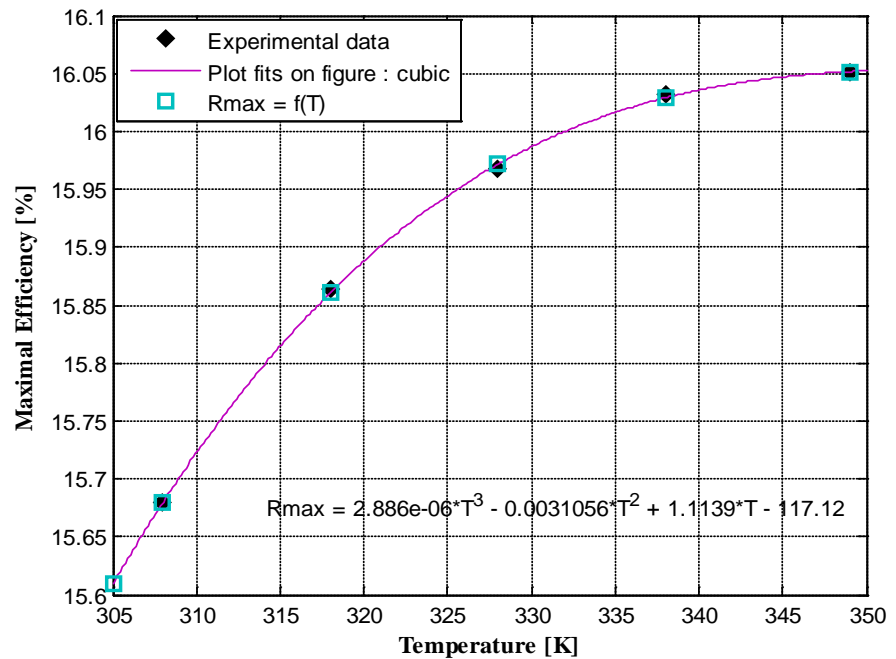


Figure 13. The maximal conversion efficiency versus temperature.

that explains a negative slope of the line. Therefore the decreasing of the photocurrent density as the temperature increases is realized.

The graphical representation of the maximal photovoltage versus temperature is given by **Figure 12**.

In **Figure 12**, the resolution of line equation provide the coefficient values $\gamma = 0.002$ mV/K and $\chi = 0.4842$ mV for a temperature of 305 K. We notice a low positive slope, it means that the photovoltage is maximal and is equal to the open-circuit voltage. The increasing of the temperature implies a minor increasing of the creation electron-hole pairs.

Figure 13 represents the variation of the maximal photovoltaic efficiency conversion as function of temperature.

These results shows that, the maximal junction recombination velocity Sf_{\max} , the maximal photovoltage and the conversion efficiency photovoltaic increase when the temperature increases, contrary the maximal photocurrent density which decreases with increasing of temperature. This shows the variation of the maximum power point as the temperature increases [34] [35]. The method in this work shows us, how to optimize the electrical power supplied by the solar cell, by use of Sf_{\max} as a research function of the maximal power point. The method is mostly based on the variation of electron diffusion coefficient in the base D, the diffusion length L, the mobility coefficient of the electron μ , the intrinsic concentration of minority carriers in the base (ni) and the recombination velocity of the charge carriers at the back side Sb all in function of temperature with the possibility to vary the thickness of the base, the electron lifetime in the base and the electron doping rate Nb. Its strength is that, its depend on the electronic structuration parameters based on the physical mechanism of solar cell, contrary

the converters and different tracking systems forcing the solar cell operating at the maximum power point (MPP) based on the macroscopic parameter of solar cell [36] [37].

3. Conclusions

In this work, after resolution the expression of the density of the minority charge carriers in excess in the base, the photocurrent density and the photovoltage, the I-V characteristic is proposed. This study shows us a decreasing of the short-circuit photocurrent and an increasing of the open-circuit photovoltage when the temperature increases. The decreasing of the short-circuit photocurrent manifests by a decreasing of the density of the excess minority carrier which crosses the junction when the temperature increases, which leads a increasing of the open-circuit photovoltage.

From the i-v characteristic of **Figure 4**, we studied the delivered electrical power by the base of the solar cell as the function of the density of minority charge carriers at the junction S_f and the photovoltage (**Figure 6** and **Figure 7**). We note that the power increases with the recombination velocity of the charge carriers at the junction S_f and of the photovoltage until a maximal value which represents the maximum power then it decreases and cancel of a values corresponding of the open-circuit photovoltage (large S_f).

A transcendental equation allowing to obtain the maximal recombination velocity of the charge carriers $S_{f_{max}}$ corresponding to the maximal power point of the solar cell is determined as the function of temperature. It depends only on phenomenological and geometrical parameters of the solar cell (L , μ , D , S_f , S_b , τ , n_i , N_b and H) and the material absorptions coefficients b_i , in the determination of the maximum power based on variation of the electron diffusion coefficient in the base as a function of temperature and the thickness H of the solar cell [18].

The transcendental equation is modeled from a simulink model (**Figure 8**), then graphically represented in **Figure 9**, and allows to extract the numerical values of $S_{f_{max}}$ for different values of the temperature noted in **Table 1**. The results in **Table 1** show that the recombination velocity of the charge carriers at the junction corresponding to the maximal power point increases, and varies with the temperature (**Figure 9**). Finally, we studied the conversion efficiency of the solar cell from the graphical values extracted of the I-V characteristic curve of **Figure 4**, then plotted I_{max} , V_{max} and η_{max} (**Figures 11-13**) as the function of the temperature compared to the $S_{f_{max}}$ values of **Figure 10** obtained from the simulink model (**Figure 8** and **Figure 9**).

References

- [1] Benmoussa, W.C., Amara, S. and Zerga, A. (2007) Optimisation du rendement d'une photopile. *Revue des Energies Renouvelables ICRESD-07 Tlemcen*, 301-306.
- [2] Gueye, S., Diallo, H.L., Ndaye, M., Dione, M.M. and Sissoko, G. (2013) *International Journal of Emerging Technology and Advanced Engineering (IJTEA)*, **3**, 1-9.
- [3] Barro, F.I., Mbodji, S., Ndiaye, M., Ba, E. and Sissoko, G. (2008) Influence of Grains

Size and Grains Boundaries Recombination on the Space-Charge Layer Thickness z of Emitter-Base Junction's n^+p-p^+ Solar Cell. *Proceedings of 23rd European Photovoltaic Solar Energy Conference and Exhibition*, 604-607.

- [4] Ndoye, S., Ndiaye, M., Diao, A., Dione, M.M., Diarisso, D., Bama, A.O.N., Ly, I., Sow, G., Maiga, A.S., Foulani, A., Barro, F.I. and Sissoko, G. (2010) Modelling and Simulating the Powering System of a Base Transmitter Station with a Standalone Photovoltaic Generator. *Proceedings of 25th European Photovoltaic Solar Energy Conference and Exhibition*, 5208-5211.
- [5] Diarisso, D., Ly, I., Sow, G., Sow, O., Gaye, I., Barro, F.I. and Sissoko, G. (2002) *Research Journal of Applied Sciences, Engineering and Technology*, **4**, 3740-3745.
- [6] Barro, F.I., Maiga, A.S., Wereme, A. and Sissoko, G. (2010) *Phys. Chem. News*, **56**, 76-84.
- [7] Sissoko, G., Correa, A., Nanema, E., Diarra, M.N., Ndiaye, A.L. and Adj, M. (1998) Recombination Parameters Measurement in Silicon Double Sided Surface Field Cell. *Proceeding of the World Renewable Energy Congress*, 20-25 September 1998, 1856-1859.
- [8] Gaye, I., Corréa, A., Ba, B., Ndiaye, A.L., Nanéma, E., Ba, A.B.B., Adj, M. and Sissoko, G. (1996) *Renewable Energy*, **3**, 1598-1601.
- [9] Ly, I., Wade, M., Diallo, H.L., EL Moujtaba, M.A.O., Lemtabott, O.H., Mbodji, S., Diasse, O., Ndiaye, A., Gaye, I., Barro, F.I., Wereme, A. and Sissoko, G. (2011) Irradiation Effect on the Electrical Parameters of a Bifacial Silicon Solar Cell under Multispectral Illumination. *Proceedings of 26th European Photovoltaic Solar Energy Conference and Exhibition*, 785-788.
- [10] Sow, O., Zerbo, I., Mbodji, S., Ngom, M.I., Diouf, M.S. and Sissoko, G. (2012) *International Journal of Sciences and Technology*, **1**, 230-246.
- [11] Corréa, A., Gaye, I., Ba, B., Ndiaye, A.L. and Sissoko, G. (1994) *Renewable Energy*, **5**, 166-168.
- [12] Madougou, S., Made, F., Boukary, M.S. and Sissoko, G. (2007) *Advanced Materials Research*, **18-19**, 303-312.
- [13] Mbodji, S., Ly, I., Diallo, H.L., Dione, M.M., Diasse, O. and Sissoko, G. (2012) *Research Journal of Applied Sciences, Engineering and Technology*, **4**, 1-7.
- [14] Zoungrana, M., Dieng, B., Lemrabott, O.H., Touré, F., Ould EL Moujtaba, M.A., Sow, M.L. and Sissoko, G. (2012) *Research Journal of Applied Sciences, Engineering and Technology*, **4**, 2967-2972.
- [15] Sissoko, G., Nanéma, E., Corréa, A., Biteye, P.M., Adj, M. and Ndiaye, A.L. (1996) *Renewable Energy*, **3**, 1848-1851.
- [16] Mbodji, S., Ly, I., Diallo, H.L., Dione, M.M., Diasseand, O. and Sissoko, G. (2012) *Research Journal of Applied Sciences, Engineering and Technology*, **4**, 1-7.
- [17] Nam, L., Rodot, M., Nijs, J., Ghannam, M. and Copppe, J. (1992) *Journal de Physique III, EDP Sciences*, **2**, 1305-1316.
- [18] Diouf, M., Gaye, S., Thiam, I., Fall, A., M, M.F., Ly, I. and Sissoko, G. (2014) *Current Trends in Technology & Sciences*, **3**, 372-375. <http://www.ctts.in/>
- [19] Kunst, M. and Sanders, A. (1992) *Semiconductor Science and Technology*, **7**, 51-59.
- [20] Zerbo, I., Koalaga, Z., Barro, F.I., Zougmore, F., Ndiaye, A.L., Diao, A. and Sissoko, G. (2004) *Journal des Sciences*, **4**, 42-46.
- [21] Furlan, J. and Amon, S. (1985) *Solid-State Electronics*, **28**, 1241-1243. [https://doi.org/10.1016/0038-1101\(85\)90048-6](https://doi.org/10.1016/0038-1101(85)90048-6)

- [22] Mohammad, S.N. (1987) *Journal of Applied Physics*, **28**, 767-772.
- [23] Sissoko, G., Museruka, C., Corr ea, A., Gaye, I. and Ndiaye, A.L. (1996) *Renewable Energy*, **3**, 1487-1490.
- [24] Sissoko, G., Sivonthanam, S., Rodot, M. and Mialhe, P. (1992) Constant Illumination-Induced Open Circuit Voltage Decay (CIOCVD) Method, as Applied to High Efficiency Si Solar Cells for Bulk and Back Surface Characterization. *11th European Photovoltaic Solar Energy Conference and Exhibition*, Poster 1B, Montreux, 12-16 October 1992, 352-354.
- [25] Diallo, H.L., Maiga, A.S., Wereme, A. and Sissoko, G. (2008) *The European Physical Journal Applied Physics*, **42**, 203-211. <https://doi.org/10.1051/epjap:2008085>
- [26] Thurmond, C.D. (1975) *Journal of the Electrochemical Society*, **122**, 133-141. <https://doi.org/10.1149/1.2134410>
- [27] El-Adawi, M.K. and Al-Nuaim, I.A. (2002) *Vacuum*, **64**, 33-36. [https://doi.org/10.1016/S0042-207X\(01\)00370-0](https://doi.org/10.1016/S0042-207X(01)00370-0)
- [28] Peykov, P. and Aceves, M. (2004) *Superficies y Vac o*, **17**, 29-31.
- [29] Thiam, N.D., Diao, A., Ndiaye, M., Dieng, A., Thiam, A., Sarr, M., Maiga, A.S. and Sissoko, G. (2012) *Research Journal of Applied Sciences, Engineering and Technology*, **4**, 4646-4655.
- [30] Ly Diallo, H., Wade, M., Ly, I., NDiaye, M., Dieng, B., Lemrabott, O.H., Ma ga, A.S. and Sissoko, G. (2002) *Research Journal of Applied Sciences, Engineering and Technology*, **4**, 1672-1676.
- [31] Ly Diallo, H., Dieng, B., Ly, I., Dione, M.M., Ndiaye, M., Lemrabott, O.H., Bako, Z.N., Wereme, A. and Sissoko, G. (2002) *Research Journal of Applied Sciences, Engineering and Technology*, **4**, 2626-2631.
- [32] Dione, B., Sow, O., Wade, M., Ibrahima, L.Y., Mbodji, S. and Sissoko, G. (2016) Experimental Processus for Acquisition Automatic Features of I-V Properties and Temperature of the Solar Panel by Changing the Operating Point. Scientific Research Publishing Inc., 3985-4000.
- [33] Na, W., Carley, T., Ketcham, L., Zimmer, B. and Chen, P. (2016) *Journal of Power and Energy Engineering*, **4**, 61-76. <https://doi.org/10.4236/jpee.2016.49006>
- [34] Diouf, M.S., Ly, I., Wade, M., Diatta, I., Traore, Y., Ndiaye, M. and Sissoko, G. (2016) *Journal of Scientific and Engineering Research*, **3**, 289-297.
- [35] Sy, K.M., Di ne, A., Tamba, S., Diouf, M.S., Diatta, I., Di ye, M., Traor , Y. and Sissoko, G. (2016) *Journal of Scientific and Engineering Research*, **3**, 433-445.
- [36] Kechar, E., Azzag, E. and Toua bia, I. (2015) *International Journal of Scientific Research & Engineering Technology*, **3**, 71-77.
- [37] Abbas, H., Abid, H., Loukil, K., Toumi, A. and Abid, M. (2013) *International Journal of Control, Energy and Electrical Engineering*, **17**, 1-6.